Available online at www.sciencedirect.com
SCIENCE DIRECT®
Medical Image Analysis 10 (2006) 71–81
MEDICAL IMAGE ANALYSIS
www.elsevier.com/locate/media

Towards a realistic echographic simulator

D. d'Aulignac [a], C. Laugier [a,*], J. Troccaz [b], S. Vieira [a]

[a] *INRIA Rhône Alpes & GRAVIR, 38330 Montbonnot, France*
[b] *TIMC-IMAG, 38706 La Tronche, France*

Received 20 May 2003; received in revised form 31 August 2004; accepted 22 February 2005
Available online 24 May 2005

Abstract

Echography is a useful tool to diagnose a thrombosis; however, since it is difficult to learn to perform this procedure, the objective of this work is to create a simulation to allow students to practice in a virtual environment.

Firstly, a physical model of the thigh was constructed based on experimental data obtained using a force sensor mounted on a robotic arm. We present a spring damper model consisting of both linear and non-linear elements. The parameters of each of these elements are then fitted to the experimental data using an optimization technique. By employing an implicit integration to solve the dynamics of the system we obtain a stable physical simulation at over 100 Hz.

Secondly, a haptic interface was added to interact with the simulation. Using a PHANToM force-feedback device may touch and deform the thigh in real-time. In order to allow a realistic sensation of the contact we employ a local modeling technique allowing to approximate the forces at much higher frequency using a multi-threaded architecture.

Finally, we present the basis for a fast echographic image generation depending on the position and orientation of the virtual probe as well as the force applied to it.

Keywords: In-vivo measurements; Physical models; Real-time simulation; Haptic interaction; Echography

1. Introduction

A very useful exam is the echography of the thigh to detect a thrombosis in the vein. A healthy vein will compress under the influence of an external force while a vein affected by thrombosis will only partially or even not at all compress, depending on the stage in the evolution of the illness. Depending on the pressure the practitioner applies with the echographic probe on the thigh, he will get an image from which the current state of the vein can be deduced, and hence a possible thrombosis diagnosed.

Motivations. However, the learning process of this procedure is somehow long and only after approximately 1000 echographic exams an acceptable competence in acquired. The first 500 exams will have to be carried out under the supervision of an experienced practitioner. Virtual environments present an alternative to the conventional medical training scheme. It is possible to create an interactive 3D simulation environment, where the doctors can manipulate or cut virtual models of organs and tissues with an haptic interface. The idea is similar to using flight simulators to train pilots. Virtual environments give an environment where there is no risk to a patient, and therefore less stressful. They are interactive and three dimensional contrary to books. Virtual environments also give a unique advantage, as it is possible to generate arbitrary anatomies and pathologies, so that the doctors can be trained for cases that are not frequently encountered.

* Corresponding author.
E-mail addresses: diego@aulignac.com (D. d'Aulignac), christian.laugier@inrialpes.fr (C. Laugier), jocelyne.troccaz@imag.fr (J. Troccaz).

1361-8415/$ - see front matter © 2005 Elsevier B.V. All rights reserved.
doi:10.1016/j.media.2005.02.001

Objectives. The goal of this work is to lay the groundwork for the development of an echographic simulator with force feedback. In the final system, the trainee will be looking at artificially generated echographic images, and interacting with a computer simulated dynamical thigh model through a haptic interface. Constructing realistic but computationally efficient models is the main challenge in developing a virtual reality training simulator. In this application it is necessary to have models for deformable tissue being manipulated by the doctor as well as models to construct artificial echographic images.

In this paper, a dynamic model of the human thigh based on experimentally determined deformation characteristics will be presented, followed by a discussion of the results and future directions.

2. Previous work

2.1. Echographic image generation

2.1.1. Generative approach

Ultrasound imaging is based on ultrasonic wave propagation inside matter. The generative approach is a physical approach consisting in modeling this propagation. Therefore, in order to generate images, we need accurate physical and geometrical models of both the probe (characteristics of emitters and receptors) and tissues to be observed. We need also a model of the interaction between the acoustic wave and the tissues. This is a very complex problem which can be tackled in several ways depending on the objectives of the simulation.

Meunier has focused on the simulation of echocardiographic image textures (Meunier, 1989). The purpose is here to be able to automatically recognize tissues from the texture analysis of the image. His study is based on Bamber and Dickinson work (Bamber and Dickinson, 1986) concerning diffuser modeling. However, generating a realistic ultrasound image needs a more complete modeling. Jensen has taken into account the ultrasonic wave behavior at interfaces and the geometry of the anatomical structures. He has generated an ultrasound image of a cyst (Jensen, 1996). The computation of this image, including only two kinds of structures, has lasted 11 h! Varlet proposes an attractive solution dealing with real-time constraints (Varlet, 1997). Firstly, a 3D model of organs is built from CT or MRI data (e.g., from the Visible Human Project) using implicit surfaces. Then, for a given position of the echographic probe, the image is generated using a ray tracing method adapted to ultrasonic rays. In order to reduce the computational time, propagation and reflection are the only acoustical properties that are considered at a purely geometric level. Texture-less images displaying the tissue interfaces are generated for echo-endoscopic applications. In these applications a major issue is to understand the topography of the organs from the echographic images to be able to monitor the difficult progression of the endoscope in the gastrointestinal track. Work is in progress to map textures onto these images. Wibaux et al. (1997) generated echographic images directly from the geometric model of the anatomy. The echographic process itself is simulated by modeling the refraction of the signal caused by the organs. In the quest for real-time performance a simplified refraction model is used to generate the images.

Generative approaches have the advantage of being applicable to any type of organs provided that a model of them is available. However, we have shown that the acoustic phenomena to be rendered are extremely complex and even simplified simulation is very time-consuming. In our context where real-time simulation is needed, a large computational time is totally prohibitive. The compromise which has been proposed by Varlet (1997) reduces the computing time but does not allow yet to generate textured images which is prohibitive for most clinical application of echography.

2.1.2. Interpolation approach

An effective alternative to the generative approach is to acquire a more or less dense 3D ultrasound volume from which images can be generated. The 3D ultrasound volume is acquired in an off-line pre-processing and images are generated during simulation, by computing a slice in the volume. Such images can be generated very rapidly. As they come from real ultrasound images, there is no realism problem. Aiger from Tel-Aviv university presents UltraSim, a commercial real-time ultrasound simulator (Aiger and Cohen, 1997) following this approach. Berlage proposes CardiAssist, a system including a simulator for training in echocardiography (Berlage, 1997). In this clinical application, the typical problems a trainee has to face are (1) to find the standard orientations of the probe relatively to the heart, (2) to detect the relevant anatomical structures in the images and (3) to learn the diagnostic content of these features. In this system, slices are computed from a pre-acquired volume of ultrasonic data and visualised. A view of a 3D model with visualization of the echographic plane is offered to the trainee for a better localization of the image.

2.1.3. Taking probe pressure into account

Further, it is possible to deform the interpolated image obtained with respect to the pressure that is applied to the probe. The criteria on which this deformation depends on includes important factors such as the arterial and venous pressure. By modifying these criteria we can simulate a set of pathologies on which medical students could be trained for the identification of the latter (Troccaz et al., 2000). UltraSim (Aiger and Cohen, 1997)

includes elastic registration tools to build a coherent volume from data acquired under different probe positions therefore involving different local deformations. Nevertheless, during simulation no deformation is applied onto the images when the computed pressure of the virtual probe varies. Varlet (1997) proposes a local non-linear model of deformation of the computed image allowing to deal with the constraints applied by the tip of the echo-endoscope to the local tissues.

The simulator we propose is based on the use of an interpolation approach to compute realistic echographic images in real-time and includes image deformation and force rendering using a physical model.

2.2. Physical modeling

However, for a meaningful echographic simulation it is of paramount importance to consider the forces involved in such a procedure since they will dictate the deformation of the tissue, and therefore, the subsequent image that is acquired.

Basdogan et al. (1996) developed an interactive 3D model of the human thigh along with a set of surgical tools to simulate procedures in virtual environments. Laffont (1997) studied the implications of the deformation of such a system, which are essential in the development of a realistic simulator coupled to a haptic interface. He based his model on a system of interconnected springs.

Mass-spring networks already been successfully applied to areas such as facial animation (Lee et al., 1995) and have the decisive advantage of being easy-to-implement and faster than finite-element simulation, even though lately considerable speed-ups have been achieved in this domain through the use of pre-calculated matrices. This has resulted in, for example, the real-time simulation with force-feedback of the human liver (Bro-Nielsen and Cotin, 1996) based on the *Visible Human* dataset. However, the model used is inconvenient in the sense that the assumption is made that the tissue is hyper-elastic and linear in its deformation. This is clearly not the case. As biomechanical experiments confirm, the stress–strain curve of human tissue is non-linear.

Lee et al. (1995) tackles this problem by using a three-layer model which takes into account the properties of the epidermis, the fatty sub-cutaneous tissue, the muscle, and the bone. The great difficulty for such a system lies in the identification of the parameters of the individual springs that will give the same results to an external force being applied as the measurements in the real world.

On the other hand, in (Pai et al., 2001) an interesting approach is taken; The model is constructed *directly* from the experimental measurements. The model is valid for linear elastic deformations, but is unable to take into account non-linear material or topology changes.

A complete survey is outside the scope of this paper. Hence please refer to (d'Aulignac, 2001)[1] for a more complete review on the real-time simulation of deformable objects.

3. Modeling of the thigh

We have constructed a dynamic model of the human thigh based on experimental measurements of its elasticity. The work presented in this section has been done in collaboration with Cenk Cavusoglu of UC Berkeley in the framework of the France–Berkeley cooperation.

3.1. Experimental setup and data acquisition

In order to model an object such that its behavior corresponds to reality, measurements must be taken on the real object. In this case we are interested in the deformation of the thigh with respect to an external force which is applied. Intuitively we can affirm that the deformation of the thigh is not the same depending on the shape of the object used to provoke this deformation, or more precisely, the contact surface of that object. Since our aim is to build a generic simulation which will allow a physically correct behavior which is almost independent of the object we choose to deform the thigh with, two different objects have been used to measure the behavior of the thigh in terms of penetration distance with respect to the external force being applied.

The first of these has a tip of pyramidal shape to provoke a punctual force response, while the second one has the same contact surface area as a typical echographic probe. These pseudo-probes are then mounted on a force sensor which in turn is mounted on a PUMA articulated arm. The probe is then positioned perpendicularly to the surface of the thigh at each of 64 points where measurements will be taken. These points are regularly distributed over the area where the echography is performed when trying to detect a thrombosis in the vein. The robotic arm then advances 2 mm using the reference of the end effector, i.e., the probe pushes along the axis which is normal to the surface of the thigh at the given point. The force is recorded and the procedure is repeated up to an upper force limit (Fig. 1).

Fig. 2(a) shows the non-linear relationship between the penetration distance and the reaction force at 11 different points along the thigh. The difference in the curves may be accounted for due to the fact that the thigh is not homogeneous and that the amount of

[1] http://www.aulignac.com/diego/work/publi.html.

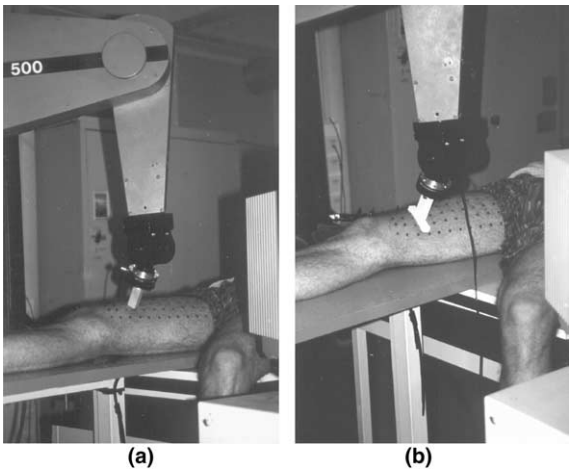

Fig. 1. The two probes used for measuring the behavior of the thigh. A probe with a punctual contact (on the left) and the pseudo-echographic probe with a larger contact surface (on the right).

the material varies with the location (e.g., in some regions fatty tissue might be pre-dominant, while in others there may be very little separating the epidermis from the bone).

Fig. 2(b) plots the values of the forces for the same points as above but using the second probe with a larger contact surface. As one might expect this results in a larger force for the same penetration distance since the external force applied is distributed over a much larger area (note that the pressure is defined as force per unit area).

The assumption is that from these two distinct sets of data it will be possible to make a model which will respond correctly to not only to the two probes used for measurement purposes, but also other probes of a different shape.

3.2. Model construction

Based on the experimental data and the computational requirements, a two layer lumped element model is chosen. Multi-layer models were also used by several authors in the literature, for example in (Lee et al., 1995) for facial animation or in (Nebel, 2001) for modeling soft tissue with volumetric finite elements.

The two layer model is composed of a surface mesh of masses, linear springs and dampers, and a set of nonlinear springs orthogonal to the surface to model volumetric effects by giving normal support to the surface mesh (see Fig. 3). At each sample point recorded in Section 3.1 we place a small mass that is attached to a nonlinear spring. The other end remains fixed (assuming the bone) at a distance perpendicularly to the surface. The force due to this nonlinear spring is given by

$$f(x) = \frac{x}{ax + b}, \tag{1}$$

where x is the change in length of the spring, i.e., the actual length minus the initial length. Hence, when a and b are positive, the magnitude of the force grows very rapidly for $x < 0$ (i.e., compression).

The linear springs on the surface give geometrical as well as numerical stability to the model. They avoid any

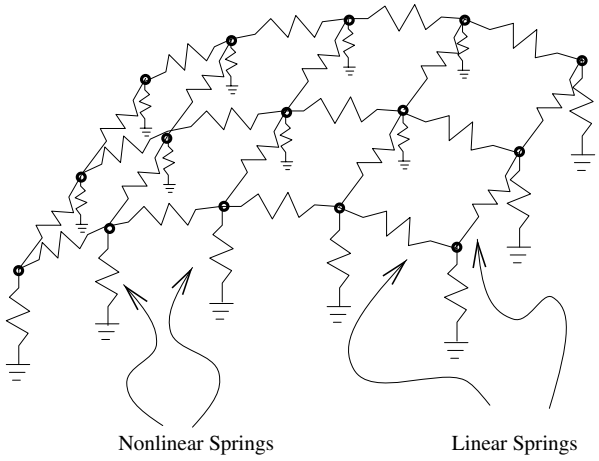

Fig. 3. Two layer model of the thigh.

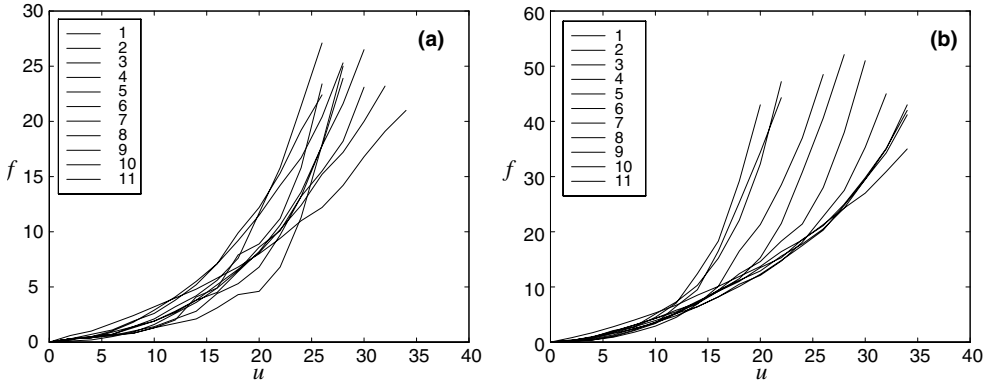

Fig. 2. Plot of the reaction force f in function of the penetration distance u at 11 different points on the thigh using a probe with a punctual contact (on the left) and the pseudo-echographic probe with a larger contact surface (on the right).

geometrical singularities in the solution as well as adding damping. The force due to each linear spring is given by

$$f(x) = \lambda x - \mu \dot{x}, \tag{2}$$

where x is the change in length of the spring, λ is the stiffness and μ the damping coefficient. The rate of the change in length is given by $\dot{x}$.

The parameters of the surface elements are uniform whereas the parameters of the nonlinear spring vary around the mesh to model the heterogeneous nature of the thigh mentioned above, while keeping the number of unknown parameters small (d'Aulignac et al., 1999a).

It should be noted that this model has been chosen ad hoc based on the experimental data available of displacement normal to the surface. Hence, its results will only be valid in compression, but not in extension.

3.2.1. Parameter estimation

Estimation of the model parameters from experimental measurements is a critical part of the modeling. Several types of methods can theoretically be used for solving this problem: an Artificial Neural Network approach requiring to make use of an adapted modeling technique (Szilas and Ronco, 1995), the Simulated Annealing (Bonomi and Lutton, 1988), the Genetic algorithms (Goldberg, 1989) which have already given some good results when identifying the physical parameters of a deformable object (see Louchet et al., 1995 and Joukhadar et al., 1997), and the Steepest Descent method (Minoux, 1983) which was used for this application.

Given that there are 64 sample points, and that at each point we have taken between 6 and 18 measurements with each probe, we obtain over 1000 different samples. Our objective is to find the parameters of our model that best describe this data. We have used a two step optimization approach based on nonlinear least squares estimation.

1. The experimental data of the indenter is first fit to a simple model without any surface elements, i.e., only the nonlinear springs.
2. The results of the previous fit is used as the initial conditions for the parameter estimation of the complete model; the parameters of the surface and nonlinear springs are adjusted in order to best match the experimental data of the indenter and the pseudo-echographic probe.

This approach is chosen to avoid problems with local minima. We have obtained better results with this method than using genetic algorithms, perhaps, as the number of parameters is small, while genetic algorithms are usually better suited for problems involving large numbers of unknowns.

One thing to note here is that the parameter estimation is based on a simplified interaction model between the tissue and probe, making the assumption that the indenter will principally act on one spring since the contact area is small, while the larger probe acts on three nodes simultaneously. In this simplified interaction model, the nodes that are not in contact with the probe are kept stationary. This is a valid assumption for the thigh, as deformations are very local.

The mean absolute error between the measured values and the values estimated by the model is 1.05 N, with standard deviation 1.84 N, over the whole dataset (i.e., all measurement samples obtained with both probes). This is equivalent to an average error of 5%. The distribution of the error can be seen in Fig. 4, showing how many of the values estimated by the model exhibit a given error with respect to the real measurements.

The few cases that give very large errors are due to inaccuracies in the measurements at some of the sample points (probably due to movement of the leg during the process). For these points there exist no parameters allowing a smooth interpolation of the data, thus resulting in large errors. Fortunately the extent of this phenomenon is limited.

3.3. Graphical model

The area of the thigh of interest for an echographic exam is relatively small as compared to the whole leg. Thus it is sufficient to model the deformation only in this area. However, to give the user an increased sense of realism and as landmarks for orientation in the virtual environment, we also render the lower leg and other side of the thigh. These are not deformable and thus the position of the vertexes will not change during simulation. It is therefore possible to transfer this data only once to the graphics hardware, and subsequently it will put only minimal demands on the CPU.

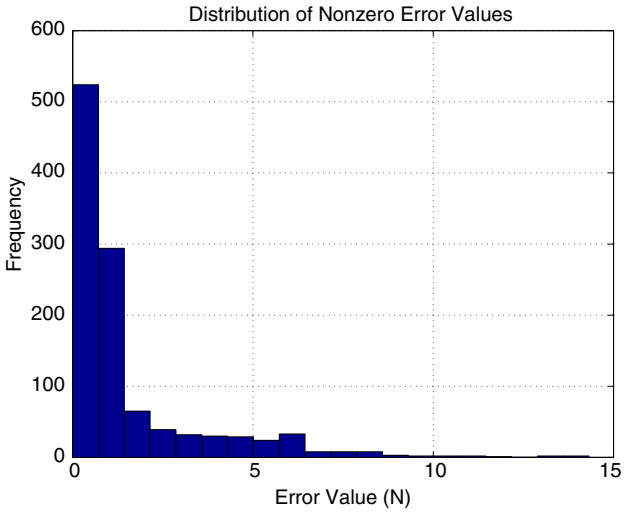

Fig. 4. Frequency distribution of the error between the measured values and the values estimated by the model.

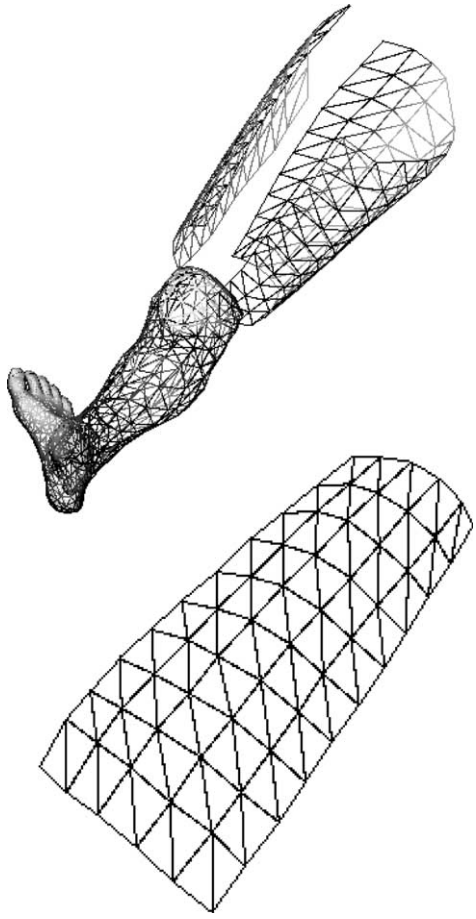

Fig. 5. Decomposition of the parts of the leg (right). The part on the left is the only part where deformation is simulated.

Fig. 5 shows how the area where deformation is simulated is integrated with the rest of the components that represent the leg only graphically. Only the linear springs on the surface are shown; the nonlinear springs are not visible in the graphical output.

4. Dynamic resolution

As discussed in (Hairer and Wanner, 1991), explicit integrations suffers from stability problems. This means that for a given timestep there is a restriction on the physical parameters that allow a stable integration. Moreover, the larger the stiffness, the smaller the timestep must be, when using explicit methods.

The stiffness values that we have estimated in Section 3.2.1 are such that the integration is not stable on our computer unless artificially large inertial values are used, i.e., large mass. This, however, leads to an unnaturally slow reaction to an external force that is applied. Further the implementation of gravitational forces is impossible. Even, higher order methods explicit methods do not allow us increase speed since the stability region does not double as we double the number of stages per timestep.

4.1. Implicit integration

Unsatisfied with explicit integration for our simulation, we have decided to investigate the suitability of implicit methods. Since speed rather than accuracy is our main concern, we have opted for the *semi-implicit* Euler method (Eq. (3)) having excellent stability (see Baraff and Witkin, 1998). For each step in the simulation the forces on the mass-points are calculated and the linear system is solved using the conjugate gradient method

$$\Delta y \left[\frac{1}{h} I - \left. \frac{\partial f}{\partial y} \right|_{y=y_{\text{rest}}} \right] = f(y_0), \tag{3}$$

where y is the state vector expressing the positions and velocities of all particles. Thus Δy represents the change in state and $f(y_0)$ the derivative at the current state. Further, I is the identity matrix and $\partial f/\partial y$ the Jacobian matrix. The accuracy of the solution is proportional to the timestep h. Higher order integration will yield better accuracy, the implicit midpoint method, for example, has a consistency of $O(h^2)$, but at a higher computational cost.

Since we only solve the linear system once per timestep, our resolution is only semi-implicit and not guaranteed to be stable for any timestep, however, it is much faster to solve and has not given us stability problems in practice.

4.2. Experimental results

Fig. 6 shows the model as it has been built in our simulation system. A force is being applied on the thigh using a probe which provokes a deformation which is in accordance with the measurements taken. The computational speed on a Silicon Graphics R10000 machine is in the order of 100 timesteps per second of animation using semi-implicit integration, which lets us envisage

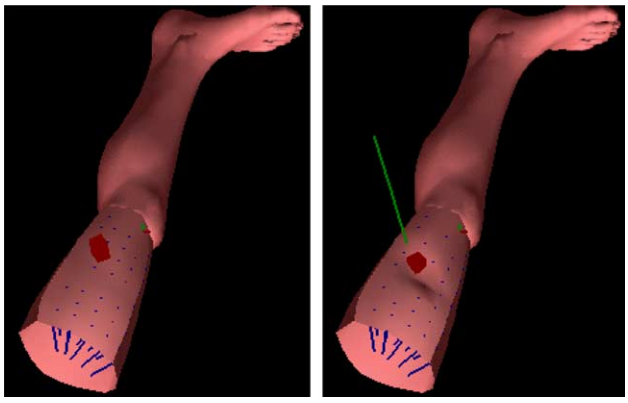

Fig. 6. Dynamic deformation of the thigh under pressure.

our simulation system as part of a working echographic simulator which operates in real-time (d'Aulignac et al., 1999b).

5. Interaction

In the previous sections the deformation of the thigh has been modeled. In this section we shall examine how to interact with the model we created using a virtual echographic probe. In Section 5.1 the collision detection and response are discussed, while the haptic force-feedback interface is detailed in Section 5.2.

5.1. Collision detection and response

The virtual echographic probe we use to interact with the model of the thigh is simple in shape, and can be modeled as a parallelepiped. However, the surface of the thigh is represented by many polygons and can become concave during interaction.

Therefore we choose to use the approach by Lombardo et al. (1999). Hence, to find the triangles of the thigh in collision with the probe, we render the surface (enabling the picking mode) in a orthogonal bounding box equivalent to the shape of the tool. This return the polygons inside the tool, i.e., in collision.

5.1.1. Distance computation

Finding the polygons of the thigh in interaction with the tool will not automatically compute the distance. We make the assumption that the tool is touching the thigh using the front side of the parallelepiped. Hence the inter-penetration distance is computed as the distance between a polygon and the front tip of the tool.

5.1.2. Collision forces

If an inter-penetration distance has been found a non-linear penalty force is calculated according to Deguet et al. (1998). This force is then distributed over the three particles of the colliding polygon using the barycentric coordinates of the point on the triangle closest to the tip of the tool.

5.2. Haptic interaction

In Section 4 we have seen that our simulation runs at approximately 100 Hz on an SGI Octane 175 Hz. This means that we check one-hundred times for the collision, calculate the appropriate penalty for a penetration (if present), and update the position of the vertexes of the deformable area according to external and internal forces each second. Even if this guarantees a stable simulation visually, i.e., at least 10 frames a second, haptic force feedback may be unsatisfactory. By this we mean that is the contact forces are transmitted to the PHANToM (distributed by SensAble Technologies) at the mentioned simulation rate, unacceptable trembling may result to the low frequency of the force update. Balaniuk (1999) proposes the use of a local approximation of the contact which we shall use in this application (Fig. 7).

5.2.1. Experimental results

As mentioned in the previous chapter, interaction forces with the simplified model are much less costly to evaluate, and, therefore, can be calculated at a much higher frequency that will give a much smoother force feedback response. Fig. 9 shows the user interactively deforming the surface of the thigh.

Fig. 8 shows the evolution of the magnitude of the force during a manipulation of the virtual thigh. Using the virtual probe we touch the thigh and slide over the

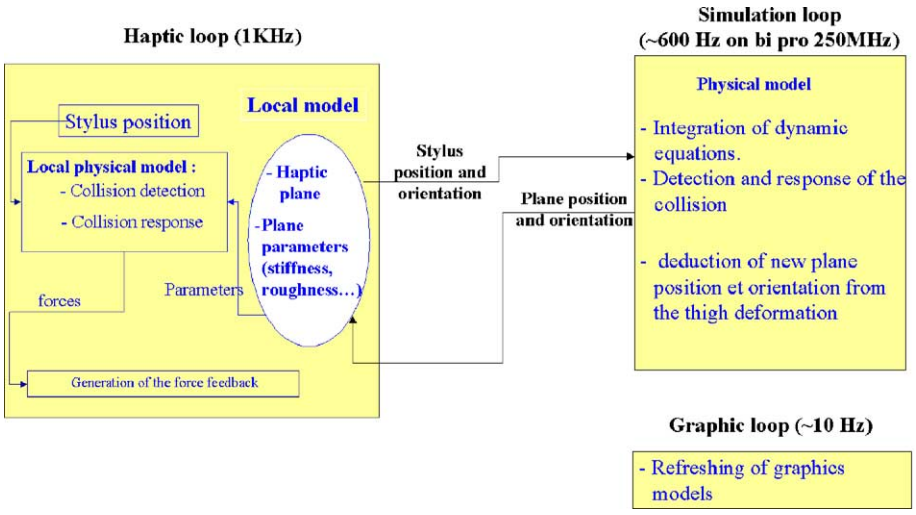

Fig. 7. Graphical overview of the two threads: the force feedback (on the left, running at 1 kHz) and the simulation (on the right).

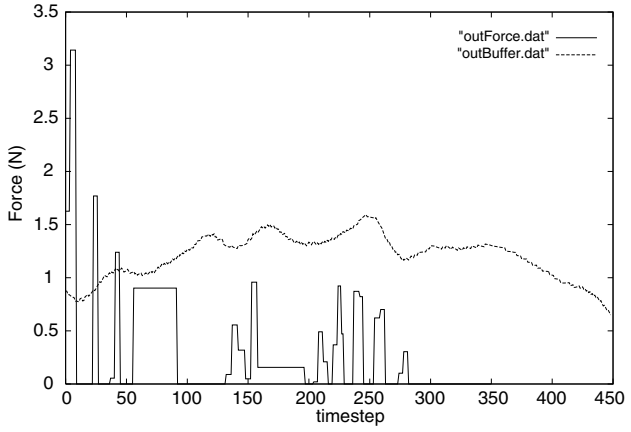

Fig. 8. Evolution of the force over a time interval using the haptic buffer model (dashed), and without (solid).

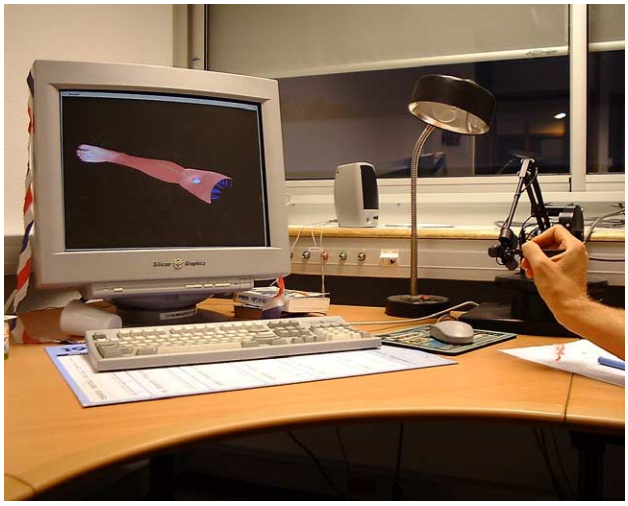

Fig. 9. The thigh model manipulated by the phantom.

surface. When using the buffer model we obtain the dashed curve. However, when attempting similar interaction without the buffer model we obtain the solid curve. This curve presents serious discontinuities; when forces return to a zero value the user has lost contact with the surface of the thigh due to the trembling. This trembling is due to the large variation of the forces (d'Aulignac et al., 2000).

5.2.2. Discussion

The local model we have implemented is a static approximation of the *contact*. By this we mean that collision detection and response are calculated using a simplified geometrical model at a much higher frequency using a multi-threaded architecture. However, the *deformation* is not modeled; the local model's parameters are constant during one step of the physical simulation (the latter calculating deformation and global collision detection).

Therefore, an interesting extension of the presented approximation the contact, would be to combine it with low order models of the deformation such as presented in (Cavusoglu and Tendick, 2000) or (Astley and Hayward, 1998).

6. Echographic image generation

As a pedagogical tool our simulator described so far is sterile. Images corresponding to the actual deformation must be generated to teach practitioner the *correlation* between deformation of the surface of the thigh and the resulting echographic image. Hence for any position and orientation of the probe on the surface of the thigh we must generate an image. Since we can not acquire nor store an infinite amount of of images for all points we will have to resort to some kind of interpolation technique. However, we must first prepare the data.

To collect this data we have taken echographic images at the same point as we have measured force–displacement curves. These echographic slices are then arranged within a bounding box (see Fig. 10) which will be divided into a 3D voxel map. The voxel map is then filled depending on the intensity of the pixels of the echographic images within each voxel. These voxels are of equilateral shape, and their size is chosen with respect to the available live memory on the machine (i.e., no swap).

Voxel map size. In this case we have used a voxel size of 0.3 mm leading to a memory requirement of approximately 120 Mb. Since the resolution of one pixel on the original echographic images is 0.1 mm there will be a small loss in resolution due to memory limitations.

Interpolation. It is clear that the for the number of sample images we have acquired the voxel map will be far from full. To fill the blank voxels we use interpolation. The TIMC laboratory has provided us with such an interpolation tool within the framework of a

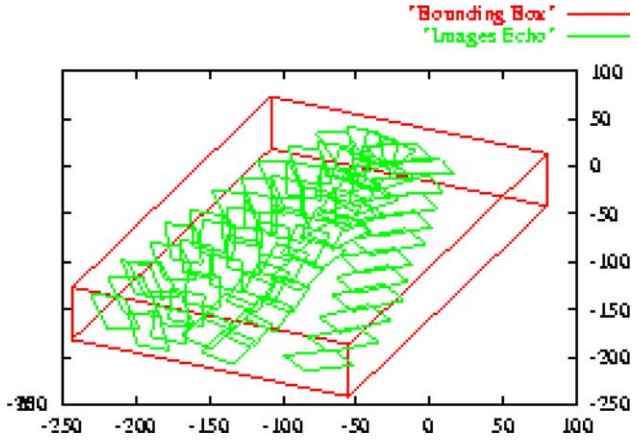

Fig. 10. Echographic slices arranged in a 3D volume.

collaboration. Thus the voxel map is filled in the preprocessing stage once and, thereafter, slices through the voxel map may be generated in real-time. The resolution of the generated image is, of course, dependent on the resolution of the voxel map (Vieira, 2000).

Once the voxel map is filled, we may calculate an image for any given position and orientation on the modeled area of the thigh. Given the data can be stored in live memory this procedure is performed in real-time.

6.1. Image deformation

Motivation. The images to construct the voxel map where acquired without deformation: the echographic probe was placed on the sample point and minimal pressure was applied to obtain the echographic image. Hence an image generated from the voxel map will be non-deformed. However, to detect a thrombosis in the thigh, the diagnosis is based on the deformation of vein. It is therefore essential for a useful simulator to take this phenomenon into account.

Problem statement. The main difficulty in modeling the deformation lies in the fact that each structure has its own way of reacting under pressure. Arteries have almost no deformation while non-pathological veins flatten. Superficial soft tissues have a near linear deformation. Deep tissues and bones have negligible deformation (Troccaz et al., 2000).

Existing approaches. The deformation of the image when pressure is applied can be obtained through the approach by Henry (1997). Given a segmentation of the undeformed echographic image to find the artery, vein, and soft tissue areas their deformation can be calculated by taking into account parameters such as arterial and venous pressure. As mentioned before, by modifying these criteria we can simulate a set of pathologies. Alternatively, a deformation function can be calculated directly from the position of features on a deformed and undeformed image. However, both these approaches rely on a segmentation having been performed previously.

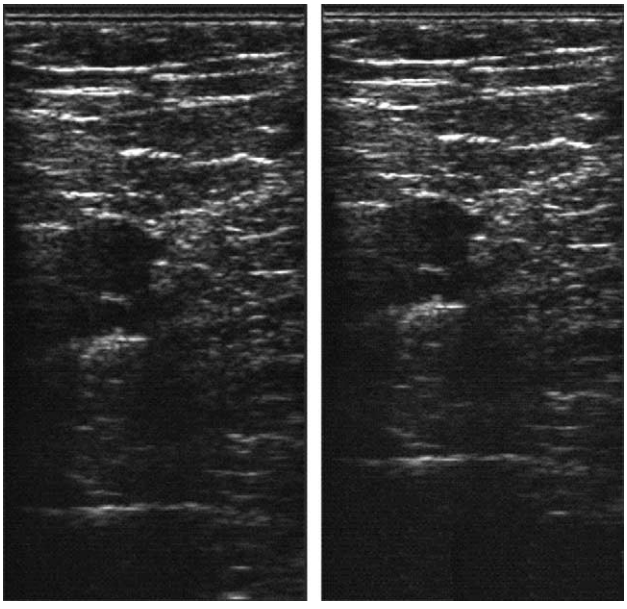

Fig. 11. Echographic images generated for a given location and orientation, with (right) and without (left) deformation.

Fig. 12. On-line generation of echographic images when interacting with the thigh using the force-feedback device. A video can be downloaded from http://www.aulignac.com/diego/work/publi.html.

Since our voxel map is not segmented into the different anatomical structures we have momentarily adopted a linear deformation regardless of the tissue. Therefore, future work on this subject should examine this problem in detail; a possiblity might be to use precalculated deformation functions as described in (Troccaz et al., 2000).

6.2. Experimental results

Fig. 11 shows how the echographic image changes as an increasing pressure is applied to the surface of the thigh by the means of the virtual echographic probe. The probe's position is given by the force-feedback device (see Fig. 12).

7. Conclusions

In this paper we have described the building blocks to prototype of an echographic simulator.

Measurements have been taken on a real human thigh using an articulated robot arm in combination with a force sensor. The force–displacement curves we have obtained on different sample points on the thigh demonstrate both the non-linear and non-homogeneous elastic nature of the material.

Furthermore, we have built a mass-spring model of the area of the thigh were the measurements were taken. The topology of this model is based on the position of

the sample points and by making assumptions on the anatomy based on the experimental data acquired. Hence, we have chosen a layered model with non-linear springs that approximate the measured force–displacement behavior. As the elasticity of the thigh is non-homogeneous a protocol of parameter identification has been installed. Using a method of steepest descent we aim to represent *all* the data samples with the lowest possible error.

To model the dynamics we have investigated the use of both explicit and implicit methods. We come to the conclusion that the overhead of solving a linear system at each time step using a semi-implicit integration is preferable to explicit integration. Because of the stiffness of the springs the latter approach is obliged to take extremely small timesteps to maintain stability.

To calculate the collision response we use the distance of penetration as a measure to calculate the penalty based response forces. However, if these forces are supplied to the force-feedback device at the rate of the physical simulation of the deformation (100 Hz using semi-implicit integration with constant Jacobian), unacceptable trembling will be the result. To remedy this problem we apply a local approximation of the contact, that will calculate the collision forces at a much higher rate (i.e., 1 kHz) in a separate program thread. This process suffices to largely improve the haptic sensation.

Lastly we have integrated our physical model with a generator of echographic images. Previous methods have interpolated images along one privileged direction of the thigh (namely the direction of the vein). Since, in this case, we want to provide an image at any position of the modeled area, we have created a voxel map based approach. The echographic images acquired at the sample points are used to partially fill the voxel map; using interpolation we then obtain a full 3D representation of the echographic data. From this voxel map, echographic images at any position or orientation can be found.

The components of the simulator have been successfully integrated in this first version. We have demonstrated that a real time production of deformable realistic echographic images and corresponding tactile feedback was possible. The following stage of this project will be its clinical testing; this means that lessons must be designed and implemented on the basis of the existing simulator to allow a beginner to experiment echographic examination and diagnosis with the simulator. The comparison of performances of learners using the simulator versus learners using traditional learning is the next stage and should demonstrate the potentiality of such tools.

Acknowledgements

We thank Cenk Cavosuglu who has been actively involved in the development of the mass-spring model of the thigh as well as the France-Berkeley Fund that made this cooperation possible. Further, we thank Etienne Dombre and Fran cois Pierrot at the LIRMM laboratory (Montpellier, France) for their kind assistance while taking the measurements at their lab. Also many thanks to Remis Balaniuk who developed the local model, and Ivan Costa for the interesting scientific discussions about the project.

Appendix A. Supplementary data

Supplementary data associated with this article can be found, in the online version at doi:10.1016/j.media.2005.02.001.

References

Aiger, D., Cohen, D., 1997. Real-time ultrasound imaging simulation. RTI.

Astley, O., Hayward, V., 1998. Multirate haptic simulation achieved by coupling finite element meshes through norton equivalents. In: Proceedings of the IEEE International Conference on Robotics and Automation, Leuven, BE, pp. 989–994.

Balaniuk, R., 1999. Using fast local modeling to buffer haptic data. In: Proceedings of the Fourth Phantom User Group Workshop – PUG99, Boston, US.

Bamber, J., Dickinson, R., 1986. Ultrasonic b-scanning: a computer simulation. Physics in Medicine and Biology.

Baraff, D., Witkin, A., 1998. Large steps in cloth simulation. In: Cohen, M. (Ed.), SIGGRAPH 98 Conference Proceedings, Annual Conference Series, ACM SIGGRAPH. Addison Wesley, pp. 43–54.

Basdogan, C., Loan, P., Rosen, J.M., Delp, S., 1996. An interactive model of the human thigh for simulating surgical procedures in virtual environments. Advances in Bioengineering ASME.

Berlage, T., 1997. Augmented reality for diagnosis based on ultrasound imagesProceedings of CVRMed-MRCAS'97, LCNS Series, vol. 1205. Springer Verlag, pp. 253–262.

Bonomi, E., Lutton, J.-L., 1988. Le recuit simulé. Pour la science, 68–77.

Bro-Nielsen, M., Cotin, S., 1996. Real-time volumetric deformable models for surgery simulation using finite elements and condensation. In: Proceedings of Eurographics, vol. 15, pp. 57–66.

Cavusoglu, M., Tendick, F., 2000. Multirate simulation for high fidelity haptic interaction with deformable objects in virtual environments. In: IEEE International Conference on Robotics and Automation, ICRA 2000, San Francisco.

d'Aulignac, D., 2001. Modélisation de l'interaction avec objets déformables en temps-réel pour des simulateurs médicaux. PhD thesis, Institut National Polytechnique de Grenoble. Available from http://www.aulignac.com/diego/work/publi.html (in English).

d'Aulignac, D., Cavusoglu, M.C., Laugier, C., 1999a. Modelling the dynamics of a human thigh for a realistic echographic simulator with force feedback. In: Proceedings of the International Conference on Medical Image Computer-assisted Intervention, Cambridge, UK.

d'Aulignac, D., Laugier, C., Cavusoglu, M.C., 1999b. Towards a realistic echographic simulator with force feedback. In: Proceedings of the IEEE-RSJ International Conference on Intelligent Robots and Systems, vol. 2, Kyongju, KR, pp. 727–732.

d'Aulignac, D., Balaniuk, R., Laugier, C., 2000. A haptic interface for a virtual exam of the human thigh. In: Proceedings of the IEEE International Conference on Robotics and Automation, vol. 3, San Francisco, CA, US, pp. 2452–2457.

Deguet, A., Joukhadar, A., Laugier, C., 1998. A collision model for deformable bodies. In: IEEE International Conference on Intelligent Robots and Systems.

Goldberg, D.E., 1989. Genetic Algorithms in Search, Optimization and Machine Learning. Addison-Wesley.

Hairer, E., Wanner, G., 1991. Solving Ordinary Differential Equations II. Springer-Verlag, Berlin.

Henry, D., 1997. Outils pour la modélisation de structure et la simulation d'examens échographiques. PhD thesis, Université Joseph Fourier, Grenoble, FR (in French).

Jensen, J., 1996. Field: A program for simulating ultrasound systems. In: 10th North-Baltic Conference on Biomedical Imaging, pp. 351–353.

Joukhadar, A., Garat, F., Laugier, C., 1997. Constraint-based identification of a dynamic model. In: Proceedings of the IEEE-RSJ International Conference on Intelligent Robots and Systems, Grenoble, FR.

Laffont, P., 1997. Simulation Dynamique Pour Le Diagnostic De Thromboses Veineuses. Mémoire De Diplôme D'etudes Approfondies. Université de Savoie, Chambéry, FR.

Lee, Y., Terzopoulos, D., Waters, K., 1995. Realistic facial modeling for animation. In: Computer Graphics Proceedings, Annual Conference Series, Proc. SIGGRAPH '95, Los Angeles, CA, ACM SIGGRAPH, pp. 55–62.

Lombardo, J.-C., Cani, M.-P., Neyret, F., 1999. Real-time collision detection for virtual surgery. In: Computer Animation, Geneva, Switzerland.

Louchet, J., Provot, X., Crochemore, D., 1995. Evolutionary identification of cloth animation models. In: Computer Animation and Simulation. Proceedings of the Eurographics Workshop.

Meunier, J., 1989. Analyse des textures d'échocardiographie bidimensionnelles du myocarde. PhD thesis, Université de Montreal (in French).

Minoux, M., 1983. Programmation mathématique - Théorie et algorithme. Collection Technique et Scientifique des Télécommunications, Dunod.

Nebel, J.-C., 2001. Soft tissue modelling from 3d scanned data. In: Magnenat-Thalmann, N., Thalmann, D. (Eds.), Deformable Avatars. Kluwer, pp. 85–97.

Pai, D.K., van den Doel, K., James, D.L., Lang, J., Lloyd, J.E., Richmond, J.L., Yau, S.H., 2001. Scanning physical interaction behavior of 3D objects. In: Computer Graphics (ACM SIGGRAPH 2001 Conference Proceedings).

Szilas, N., Ronco, E., 1995. Action for learning in non-symbolic systems. In: European Conference on Cognitive Science, Saint Malo, France.

Troccaz, J., Henry, D., Laieb, N., Champleboux, G., Bosson, J.L., Pichot, O., 2000. Simulators for medical training: application to vascular ultrasound imaging. Journal of Visualization and Computer Animation.

Varlet, E., 1997. Etude d'un simulateur pédagogique d'écho-endoscopie digestive, modélisation et réalisation. PhD thesis, Université Sciences et Techniques de Lille (in French).

Vieira, S., 2000. Intégration de modéles déformables avec un générateur d'images échographiques. Technical report, Diplome d'Ingenieur, Conservatoire National des Arts et Metiers (in French).

Wibaux, L., Varlet, E., Chaillou, C., 1997. Contruction d'images échographique pour des simulateurs medicaux. In: 5eme Journées AFIG 97.